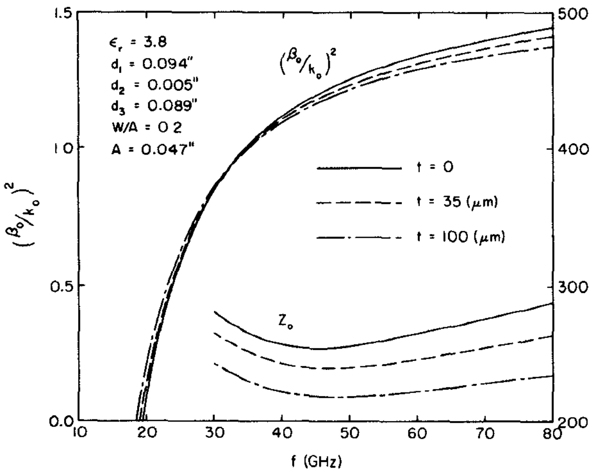

Fig. 6. Propagation characteristics of unilateral finline.

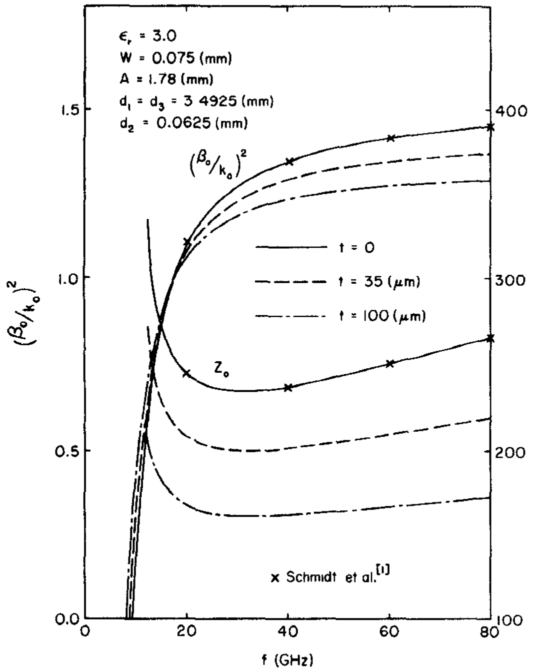

Fig. 7. Propagation characteristics of bilateral finline.

filled dielectric waveguide both for the finite and zero thickness of the metallization. However, when our results are compared with the published data by Beyer [4], some discrepancies are noted. The values obtained by Beyer are larger than those for the case of infinitely thin metallization ($t = 0$), and they do not appear to converge to a correct limiting value as W approaches A, as they should.

Fig. 6 shows the frequency dependence of the effect of the metallization thickness on the effective dielectric constant, and on the characteristic impedance in a unilateral finline. The finite thickness reduces the propagation constant in the higher frequency range as it does in the open slot line [5], because in these frequency ranges the fields are concentrated near the gap in the finline and it acts similar to an open slot line. In contrast, a finline behaves as a ridged waveguide near the cutoff frequency, and consequently, the thicker its diaphragm, the lower its cutoff frequency [7].

Fig. 7 shows the effect of the metallization thickness of a bilateral finline. The results for the limiting case of $t = 0$, i.e., zero metallization thickness, are compared with those published by Schmidt and Itoh [1], and the agreement is quite good.

IV. Conclusions

In this paper, the hybrid mode formulation was used to analyze finline structures with finite metallization thicknesses. This formulation used in conjunction with the equivalent circuit analysis is considerably simpler than the conventional Green's function approach. This method itself is quite general and can be applied to different types of finline structures by a simple modification of equivalent circuits which can be obtained easily.

Numerical results are presented to show the effects of finite metallization thickness on the propagation characteristics of unilateral and bilateral finline structures.

References

[1] L. P. Schmidt and T. Itoh, "Spectral domain analysis of dominant and higher order modes in fin-lines," *IEEE Trans. Microwave Theory Tech.*, vol. MTT-28, pp. 981–985, Sept. 1980.

[2] L. P. Schmidt, T. Itoh, and H. Hofman, "Characteristics of unilateral fin-line structures with arbitrary located slots," *IEEE Trans. Microwave Theory Tech.*, vol. MTT-29, pp. 352–355, Apr. 1981.

[3] Y. Hayashi, E. Farr, S. Wilson, and R. Mittra, "Analysis of dominant and higher-order modes in unilateral finlines," *Arch. Elek. Übertragung.*, vol. 37, no. 3/4, pp. 117–122, Mar.–Apr. 1983.

[4] A. Beyer, "Analysis of characteristics of an earthed finline," *IEEE Trans. Microwave Theory Tech.*, vol. MTT-29, pp. 676–680, July 1981.

[5] T. Kitazawa, Y. Hayashi, and M. Suzuki, "Analysis of the dispersion characteristic of slot line with thick metal coating," *IEEE Trans. Microwave Theory Tech.*, vol. MTT-28, pp. 387–392, Apr. 1980.

[6] T. Kitazawa, Y. Hayashi, and M. Suzuki, "A coplanar waveguide with thick metal coating," *IEEE Trans. Microwave Theory Tech.*, vol. MTT-24, pp. 604–608, Sept. 1976.

[7] J. R. Pyle, "The cutoff wavelength of the TE_{10} mode in ridged rectangular waveguide of any aspect ratio," *IEEE Trans. Microwave Theory Tech.*, vol. MTT-14, pp. 175–183, Apr. 1966.

An Evanescent Mode Waveguide Bandpass Filter at *Q* Band

N. P. AKERS AND P. D. ALLAN

***Abstract*—Evanescent-mode filters have previously been restricted in frequency to *X* band or below. Here, the performance of an evanescent-mode waveguide bandpass filter with a center frequency in the 26–40-GHz band (*Q* band) is reported.**

I. Introduction

The design principles of evanescent-mode waveguide filters have been developed over a number of years by Craven, Mok, [1]–[3] and others [4], [5]. Initially, those principles were based on image parameter theory but a more refined technique was later developed which employed equivalent circuits to accurately represent the below-cutoff guide and its obstacles.

Manuscript received November 2, 1983; revised May 31, 1984.

N. P. Akers was with M.S.D.S., Ltd., Frimley, Surrey, U.K. He is now with the Department of Electrical and Electronic Engineering, Portsmouth Polytechnic, Portsmouth, Hampshire, U.K.

P. D Allan is with M.S.D.S Ltd., Grimley, Surrey, U.K.

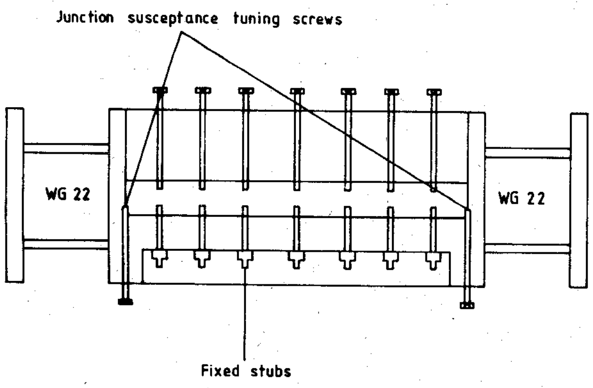

Fig. 1. Realization of seven-element Q band filter.

The advantages of evanescent-mode filters over more conventional waveguide filters are their lightness and small volume. They can be designed to couple directly into either coaxial transmission line or above cut-off propagating waveguide, and volume can be traded off against insertion loss by an appropriate choice of evanescent-mode waveguide size.

So far, the practical use of evanescent-mode waveguide filters has been confined to relatively low microwave frequencies where the use of conventional waveguide filters may be prohibited by considerations of size. This paper presents the performance of a bandpass filter designed with the following initial specifications:

a) a center frequency f_0 in Q band (26–40 GHz),
b) 10-percent bandwidth,
c) 40 dB of rejection 1 GHz outside the passband,
d) 0.1-dB amplitude ripple within the passband.

The theoretical performance of the filter is predicted and the prediction compared with the measured performance of a filter designed to achieve the above performance.

II. Practical Filter Design

A diagram of a seven-element Q band filter designed using the theory of Craven and Mok [3] is shown in Fig. 1. Waveguide 25 was chosen as the evanescent waveguide in order to keep the insertion loss low, and the filter was designed to couple into and out of propagating waveguide 22. The junction susceptance between the two waveguides was tuned by means of screws positioned at the input and output ports. Minimum loss is achieved by the use of a high-conductivity material and so the body of the device was constructed of copper waveguide and the screws were of copper-plated brass.

An important condition for achieving low loss in an evanescent-mode filter is good electrical contact between the capacitive obstacles and the waveguide walls at, or as close as possible to, the inner surface of the waveguide. This becomes progressively more difficult to achieve with tuning screws as the dimensions of the evanescent-mode waveguide are reduced. The problem was overcome by the use of fixed stubs soldered to the waveguide as the capacitive obstacles with fine tuning achieved by screws positioned over each stub. Each fine-tuning screw had its thread turned off for that part of its length which penetrated into the waveguide. When tuning was completed, each tuning screw was fixed in place by a laterally positioned clamping screw. Overall length of the filter, including waveguide 22 flanges, was 3.7 cm.

III. Filter Performance

The transmission loss response curve for the filter is shown in Fig. 2, with the frequency scale normalized to the center frequency f_0. Within the passband, the insertion loss was less than or equal to 1 dB, which compares favorably with the predicted response which is also shown in Fig. 2. The rejection loss response is shown in Fig. 3 with the computed curve again given for comparison. The out-of-band rejection (1 GHz out of band) was higher on the lower frequency side ($\sim$ 35 dB) than on the higher ($\sim$ 24 dB). This was probably due to the fact that the frequency above the passband was approaching the cut-off frequency of waveguide 25 (39.9 GHz). In-band amplitude ripple was less than 0.3 dB and there were no spurious responses within Q band.

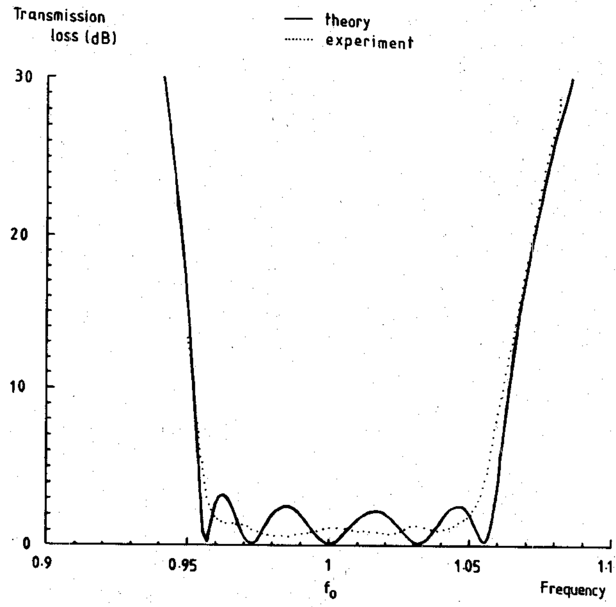

Fig. 2. Experimental and theoretical transmission loss.

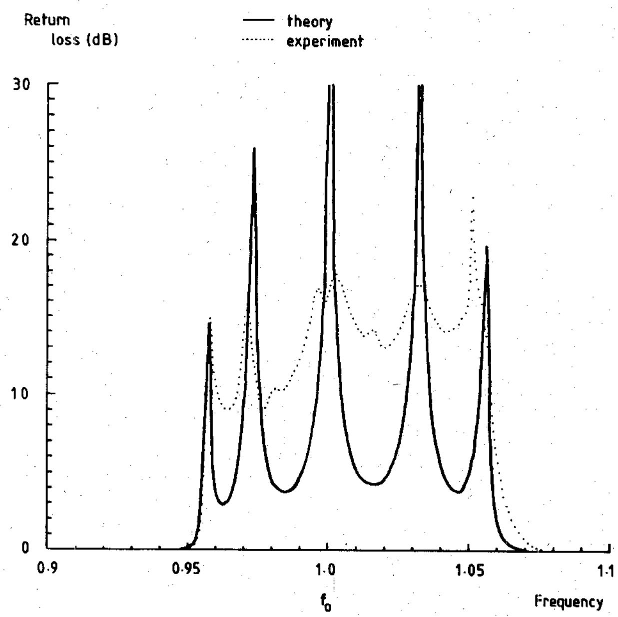

Fig. 3. Experimental and theoretical return loss.

IV. Conclusions

Improvements in insertion loss and out-of-band rejection should be possible by replacing the metal resonators with resonators of a suitable dielectric. Refinements in the analysis to take account of the junction susceptance also should result in improved performance.

By the very nature of the device, it is not possible for evanescent-mode waveguide filters to be produced with center frequencies much above Q band. The waveguide dimensions and resonator lengths are so small that machining tolerances become the limiting factor. It has been shown, however, that at frequencies up to Q band, the advantages of evanescent-mode filters, of lightness and compactness, and simplicity of design and construction are readily achievable.

Acknowledgment

The authors gratefully acknowledge the contribution made to this study by Dr. J. Howard and would like also to thank G. Craven for much helpful advice.

References

[1] G. Craven, "Waveguide bandpass filters using evanescent modes," *Electron. Lett.*, vol. 2, no. 7, pp. 251–252, 1966.

[2] G. Craven "Waveguide below cutoff: A new type of microwave integrated circuit," *Microwave J.*, vol. 13, no. 8, pp. 51–58, 1970.

[3] G. Craven and C. K. Mok, "The design of evanescent mode waveguide bandpass filters for a prescribed insertion loss characteristic," *IEEE Trans. Microwave Theory Tech.*, vol. MTT-19, no. 3, pp. 295–308, 1971.

[4] W. A. Edson, "Microwave filters using ghost-mode resonance," in *I.R.E. Electronic Components Conf. Proc.*, 1961, pp. 19-1–19-12.

[5] R. V. Snyder, "New application of evanescent mode waveguide to filter design," *IEEE Trans. Microwave Theory Tech.*, vol. MTT-25, pp. 1013–1021, Dec. 1977.

[6] W. W. Mumford, "Maximally-flat filters in waveguide," *Bell Syst. Tech. J.*, vol. 27, p. 684, 1948.

Extension of Levy's Large-Aperture Design Formulas to the Design of Circular Irises in Coupled-Resonator Waveguide Filters

A. JENNINGS, MEMBER, IEEE, AND R. L. GRAY

Abstract—This paper extends some results for waveguide irises to obtain accurate design formulas for the design of circular waveguide irises in coupled-resonator rectangular waveguide filters. Experimental results confirm the improved accuracy of the new design formulas.

The new approach has been successfully applied to the design of a 12-GHz waveguide filter in WR90 waveguide for satellite transponder studies. Improved accuracy in the iris design enabled the filter to meet stringent group delay specifications.

I. Introduction

A waveguide coupled-resonator filter typically consists of a number of half-wavelength sections coupled via irises in the resonator walls, as illustrated in Fig. 1(a). When stringent specifications are placed on the filter, the need arises for accurate design of the irises. In the course of development of a filter for satellite transponder studies [1], existing methods of design were found to be inadequate, especially for the cases where the iris diameters are an appreciable fraction of the wavelength and the thickness t of the iris is significant.

The iris coupling is described by the equivalent circuit of Fig. 1(b) and the coupling coefficient k is expressed as

$$k = \frac{L_i}{L + L_i} \tag{1}$$

where L_i is the equivalent inductance of the iris [6].

Manuscript received November 21, 1983; revised June 1, 1984.

The authors are with Telecom Australia Research Laboratories, 762–772 Blackburn Rd., Clayton North, Melbourne, Vic. 3168, Australia

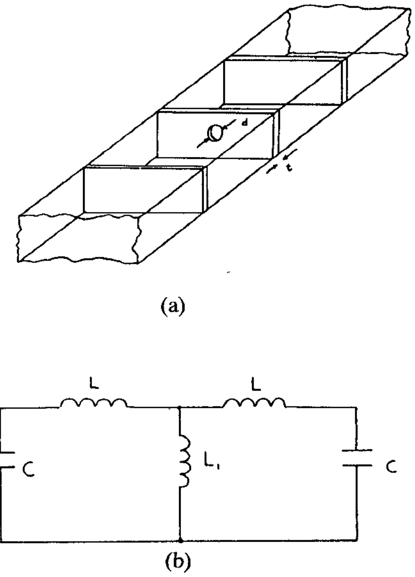

Fig. 1. (a) Iris coupling, and (b) equivalent circuit.

II. Calculation of the Iris Coupling Coefficient

For the case of small irises in thin walls, the coupling coefficient can be related to the iris diameter and the cavity dimensions in terms of simple formulas [2], [3]. Cohn [4] treats the case of large irises by employing empirical correction factors for the iris size and the wall thickness. Levy [5] has extended and applied these results to the design of multiaperture directional couplers.

McDonald [6], [7] has derived exact correction factors for wall thickness, removing the need for an empirical correction factor. Levy [9] has recently combined the results of Cohn and McDonald to give more accurate design methods for multiaperture directional couplers. In the following, Levy's results are extended to the cases of waveguide–cavity coupling and cavity–cavity coupling. This yields accurate design formulas for the irises of multicoupled waveguide filters.

The magnetic polarizability of the iris is defined as the ratio of source strength induced in the coupled cavity to incident field at the iris [2], [3]:

$$\underline{P} = -M\underline{H}_t \tag{2}$$

$\underline{P}$ magnetic dipole moment induced in the coupled cavity,
$\underline{H}_t$ tangential magnetic field incident at the iris,
M magnetic polarizability.

It can be shown [3, p. 462] that the coefficient of coupling between two cavities coupled via an end-wall iris (Fig. 2(a)) is

$$k_e = \frac{M\lambda^2 s^2}{l_1^3 ab} \tag{3}$$

λ free-space wavelength,
λ_g guide wavelength,
$l_1 = \frac{s\lambda_g}{2}$ s integer.

Similarly, the coefficient of coupling between two cavities coupled via a side-wall iris (Fig. 2(b)) is [3, p. 462]

$$k_s = \frac{M\lambda^2}{l_1 a^3 b}. \tag{4}$$